2001

Indoor radio channel of bluetooth technology

Kai Hock Charlie Khoo
Edith Cowan University

Indoor Radio Channel

Of

Bluetooth Technology

A Thesis Submitted in Partial Fulfilment of
The Requirements for the Award of
Bachelor of Engineering (Communication Systems)

Khoo Kai Hock Charlie

Faculty of Communications, Health and Science
Edith Cowan University
Western Australia

Date of Submission : 9 Feburary 2001

Edith Cowan University

Copyright Warning

You may print or download ONE copy of this document for the purpose of your own research or study.

The University does not authorize you to copy, communicate or otherwise make available electronically to any other person any copyright material contained on this site.

You are reminded of the following:

- Copyright owners are entitled to take legal action against persons who infringe their copyright.

- A reproduction of material that is protected by copyright may be a copyright infringement. Where the reproduction of such material is done without attribution of authorship, with false attribution of authorship or the authorship is treated in a derogatory manner, this may be a breach of the author's moral rights contained in Part IX of the Copyright Act 1968 (Cth).

- Courts have the power to impose a wide range of civil and criminal sanctions for infringement of copyright, infringement of moral rights and other offences under the Copyright Act 1968 (Cth). Higher penalties may apply, and higher damages may be awarded, for offences and infringements involving the conversion of material into digital or electronic form.

USE OF THESIS

The Use of Thesis statement is not included in this version of the thesis.

DECLARATION

I certify that this thesis does not, to the best of my knowledge and belief:

i   incorporate without acknowledgment any material previously submitted for a degree or diploma in any institution of higher education;

ii   contain any material previously published or written by another person except where due reference is made in the text; or

iii   contain any defamatory material.

Signature: _____

Date: _____ 9 / 2 / 2001 _____

TABLE OF CONTENTS

FIGURES AND TABLES

List of Figures

List of Tables

ACKNOWLEDGEMENT

Project Supervisor: Dr. Stefan Lachowicz

I would like to express my sincere gratitude to my supervisor, Dr. Stefan Lachowicz and MMC project supervisor, Dr. Ma Zhong Ming for their advice and guidance for this project. Dr. Stefan had given constructive and practical recommendations on my project during my visit to the university and his trip in Singapore. Dr. Ma had always been around when I needed help. I am grateful for their time spent with me despite their busy schedule.

I am also very gratified to my colleague, Mr. Lee Chye Hup and my manager, Mr. Ho Siew Foo for their understanding and help. Lee had been very supportive and willingly to loan me the test and measurement equipments. Ho had been obliging to approve my urgent leaves and not being able to stay over time for meetings.

My thanks are also due to the librarians at Ngee Ann Polytechnic, who kindly guided me on how to speed up the searching time for related IEEE journals.

Last but not least, I would like to thank my family and friends who have inspired me and given me unfaltering support throughout my education career.

Khoo Kai Hock Charlie

ABTRACT

This thesis discusses the findings of the final year project involving the characterisation of indoor radio channel specified by Bluetooth technology through theoretical analysis, simulations and actual measurements through field experiments.

The concepts of indoor radio propagation effects and its statistical models are explored. Inaddition, Bluetooth specifications are also studied and presented in Section 1. These provided a clear understanding of the radio propagation behaviour inside a building and the radio performance of Bluetooth specifications. Profound understanding of the propagation characteristics of the indoor radio channel is a major requirement for successful design of any indoor wireless communication systems. The knowledge is used here to investigate Bluetooth radio performance. Detailed characterisation of indoor radio channel is studied and presented in section 2.

Path loss model and amplitude fading model are used in the theoretical analysis, simulations and field experiments have been done to characterise the indoor channel. Field experiments and its measurements were performed and recorded to verify against the simulated results. Attenuation factor of various materials were measured since it is a critical component effecting the path loss calculation. These are presented in section 3.

PROJECT DEFINITION

Aim

The aim of the project was to conclude the limitation of the radio link performance by conducting analysis, simulations and experiments on the indoor radio channel for the Bluetooth technology.

The objectives of the project were:

- An understanding of the Bluetooth specifications.

- An understanding of the indoor multipath propagation.

- Design, analysis and simulation of the small-scale fading and path loss model in Matlab and theory.

- Analyse the link budget of Bluetooth device given the usage and specifications.

- An understanding and usage of the signal generator and spectrum analyser.

Scope

The project has both the research component and experiment (verification) component to study and investigate the performance of the radio link of the Bluetooth indoor radio channel.

- Strong understanding of the indoor multipath propagation is required to appreciate the indoor radio channel characteristics and its statistical models.

- Bluetooth specifications were studied and mapped it into the indoor radio channel. Since the technology is relatively new and expert personals are rare, a lot of time

was spent to understand the specifications. The only knowledge source is mainly reading from the Internet.

- With limited resources on the availability of test and measurement equipment, CW (Continuous Wave) signal experiments were conducted to verify and test the limitation of the radio link budget. Also to measure the attenuation factor of objects found in the office. Signal generator and spectrum analyser were the only available equipment.

- Matlab programming was done to obtain the simulation results. The results were then compared with the field experiment results.

- Crash course on the usage of the signal generator and spectrum analyser by experienced engineer proved more useful and effective than reading the manuals.

1 BLUETOOTH TECHNOLOGY

1.1 Introduction

The name Bluetooth comes from a Danish Viking and King, Herald Blatand (Bluetooth in English), who live in the latter part of the 10th century. He united and controlled Denmark and Norway. The Bluetooth Special Interest Group (SIG) was launched in May 1998 by the founding companies, Ericsson Mobile Communications, Intel, IBM, Toshiba and Nokia Mobile Phones. The intention of the Bluetooth SIG is to form a de facto standard for air interface and the software that controls it. The purpose is to achieve interoperability between different devices from different producers of portable computers, mobile phones and other devices. Bluetooth is a point-to-point or point-to-multipoint short-range radio link solution. It was created to enable many different usage models from ad hoc networking to cable replacement. It is one of the emerging standards to provide RF connectivity for both existing and upcoming fixed and mobile devices. Its key features are robustness, low complexity, low power and low cost. Its applications are capable of data and voice communication. For example, imagine that in the conference room, business cards are exchanged wirelessly amongst the participants using notebook computers, Personal Digital Assistance (PDA) and handphones. Further imagine that when you are driving down the road, although your hands are busy controlling the wheels you can still answered calls from a headset that is wirelessly connected to your handphones.

Indoor Radio Channel of Bluetooth Technology

1.2 Overview

Generally, the Bluetooth system consists of a radio unit, a link control unit and a support unit for link management and host terminal interface functions. The Bluetooth link controller carries out the Baseband protocols and other low-level link routines. Link layer messages for link set-up and controls are defined in the link manager protocol.

Detailed description on the radio specifications are presented since it is required to map into the indoor radio channel. Furthermore, the baseband and network topology are also included to help investigation on the radio performance. Overviews on the rest of the specifications are also provided here.

Figure 1.1: Overview on the Bluetooth System (Specification of the Bluetooth System-Core v1.0B, 1999)

1.2.1 Bluetooth Core

There are two volumes in the Bluetooth Specification V 1.0B, the Core and the Profiles. The Core specification addresses how the technology works (that is, the Bluetooth protocol architecture). The Profiles specification describes how the technology is used (i.e. how different models in the Core can be implemented in the various applications

Khoo Kai Hock Charlie   Thesis on Final Year Engineering Project, 2001.

mentioned in the Profiles.). From the Core specifications, the complete protocol stack is summarised and shown in *figure 1.2*.

Figure 1.2: Overview of the Bluetooth Core Specifications (Specification of the Bluetooth System-Core v1.0B, 1999)

(It comprises of both Bluetooth and adopted (non-Bluetooth) protocol stacks. Adopted Protocols are those shaded in grey.)

1.2.1.1 Link Manager Protocol, LMP

The Link manager Protocol, LMP, is responsible for link set-up between Bluetooth units. It handles the control and negotiation of packet size used when transmitting data. LMP also handles management of power modes, power consumption and state of a Bluetooth

unit in a piconet. Finally, this layers handle the generation, exchange and control of links and security of links, which are the encryption keys for authentication and encryption. LMP also provides a mechanism for measuring the QoS (Quality of Service) and RSSI (Received Signal Strength Indication).

1.2.1.2 Host Controller Interface, HCI

Host Controller Interface (HCI) is an interface that gives higher-level protocols the possibility to access lower layers. Control of the Baseband Controller and Link Manager and access to hardware status and control registers is achieved by using commands that is provided by the HCI. Exchange of commands and data is made between the HCI driver on the host and the HCI firmware on the Bluetooth hardware. The Host Controller Transport Layer provides both HCI layers ability to exchange data with each other. When an HCI event occurs, the Host will notice this irrespective of which Host Controller Transport Layer that was used. When an event has occurred the host will analyse the received packet to decide which event it was.

1.2.1.3 Logical Link Control and Adaptation Protocol, L2CAP

Logical Link Control and Adaptation Protocol (L2CAP) is a protocol that supports higher level protocol multiplexing, packet segmentation and re-assembly, the maintenance of QoS and group management. L2CAP is placed above the Baseband protocol and interfaces with higher protocols like Service Discovery Protocol, RFCOMM and Telephony Control Protocol. All protection of the transmitted information (integrity

checks etc.) is done at Baseband level. The L2CAP layer provides connection-oriented and connectionless data services to upper layers. The L2CAP must be able to determine the Bluetooth address of the device that sends the commands.

1.2.1.4 Service Discovery Protocol, SDP

The Service Discovery Protocol (SDP) defines how a Bluetooth client's application shall act to discover available Bluetooth server's services and their characteristics. The protocol defines how a client knows anything of the available services. The SDP provides means for the discovery of new available services when the client enters the area where a Bluetooth server is operating. The SDP also provides functionality for detecting when a service is no longer available. SDP can only be used for searching for services and collecting information about them, by accessing their attributes and associated service access protocols. It does not provide any means of accessing services. negotiating service parameters, billing etc. However, in later versions we may see these functions as part of SDP. SDP can function over a reliable packet transport (or even unreliable. if the client implements timeouts and repeats requests as necessary).

1.2.1.5 RFCOMM

RFCOMM is intended as a cable replacement protocol. The protocol covers applications that make use of the serial ports of the unit. RFCOMM emulates RS 232 control and data signals over the L2CAP channels. It provides services to higher layers, for example, Point-to-Point Protocol (PPP), Object Exchange protocol (OBEX) and AT Commands.

1.2.1.6 Audio

Audio transmissions can be performed between one or more Bluetooth devices, using many different usage models. Audio data do not go through the L2CAP layer but go directly, after opening a Bluetooth link and a straightforward set-up, between two Bluetooth units.

1.2.1.7 Telephony Control Protocol, TCS BIN

The Telephony Control protocol – Binary, TCS Binary or TCS BIN, is a bit oriented protocol, which defines the call control signalling for the establishment of speech and data calls between Bluetooth units. TCS BIN also provides functionality to exchange signalling information unrelated to ongoing calls. The TCS BIN is based on the ITU-T Recommendation Q.931.

1.2.2 Bluetooth Profiles

Figure 1.3 shows the overview of the Bluetooth Profiles. The Bluetooth cable replacement protocol is RFCOMM and the Telephony Control Protocol is Binary, TCS Binary or TCS BIN.

Figure 1.3: Overview of the Bluetooth Profile Specifications (Specification of the Bluetooth System-Core v1.0B, 1999)

The Bluetooth Profiles specify how the interoperability solution for the functions described in the usage models should be provided using protocols. In the Bluetooth Specification volume, Profiles, there are four general profiles defined, on which some of the highest prioritised user models and their profiles are directly based on. The four models are:

1. Generic Access Profile (GAP)

2. Service Discovery Application Profile (SDAP)

3. Serial Port Profile

4. Generic Object Exchange Profile (GOEP)

A number of usage models are identified by the Bluetooth SIG as fundamental. and are therefore. highlighted in the Bluetooth documentation. For every user model there is one or more corresponding profiles.

1.2.2.1 Generic Access Profile, GAP

The Generic Access Profile. GAP. defines how two Bluetooth devices discover and establish a connection with each other. GAP handles discovery and establishment between units that are unconnected. The GAP describes the common modes used by all other profiles. it ensures that devices can establish contact with each other independent of which application profile supported. The main purpose is to describe how the lower layers (link controller and link manager protocol) are used. Other aspects are security-related issues and description of higher layers.

1.2.2.2 Service Discovery Application Profile, SDAP

The Service Discovery Application Profile. SDAP. defines the investigation of services available to a Bluetooth unit. The profile handles the search for known and specific services as well as general service search. The SDAP is dependent on the GAP. as SDAP re-uses parts of the GAP.

1.2.2.3 Serial Port Profile

The Serial Port Profile defines how to set-up virtual serial ports on two devices and connecting these with Bluetooth. Using this profile provides the Bluetooth units with an emulation of a serial cable using RS232 control signalling. The profile ensures that data rates up to 128 kbit/s can be used. The Serial Port Profile is dependent on the GAP, just as SDAP, Serial Port Profile re-uses parts of the GAP.

1.2.2.4 Generic Object Exchange Profile, GOEP

The Generic Object Exchange Profile, GOEP, defines the set of protocols and procedures to be used by applications handling object exchanges. A number of usage models, described in the section Bluetooth Usage Models, are based on this profile, for example, File Transfer and Synchronisation. Typical Bluetooth units using this profile are notebook Personal Computers, Personal Digital Assistance, mobile phones and smart-phones. The GOEP is dependent on the Serial Port Profile.

1.3 Radio Specifications

SIG has launched a campaign to reach total harmonisation of the frequency band. This is to ensure interoperation of all Bluetooth devices in any parts of the world, achieving a truly a global standard. Many electronic devices are operating on the ISM band and microwave ovens are the strongest source of interference. To combat this, frequency-hopping (FH) and short data packets are employed. The frequency hopping scheme is set up to 1600 hops per second over 79 one MHz channels and is used to spread over the

entire available ISM spectrum. Spread spectrum technology is used to operate in noisy environments and to allow multiple piconets to co-exist without a noticeable loss in throughput.

A low transmitter power of 0dBm is used to operate in the range of 10m. However, it is possible to extend to 100m using the 20dBm transmitter. The equipment is classified into three power classes as shown in *table 1.1*.

Power Class	Maximum Output Power (Pmax)	Nominal Output Power	Minimum Output Power[1]	Power Control
1	100 mW (20 dBm)	N/A	1 mW (0 dBm)	Pmin<+4 dBm to Pmax Optional: Pmin[2] to Pmax
2	2.5 mW (4 dBm)	1 mW (0 dBm)	0.25 mW (-6 dBm)	Optional: Pmin[2] to Pmax
3	1 mW (0 dBm)	N/A	N/A	Optional: Pmin[2] to Pmax

Table 1.1: Equipment Power Classes (Specification of the Bluetooth System-Core v1.0B, 1999)
Note 1). Minimum output power at maximum power setting.
Note 2). The lower power limit Pmin <-30dBm is suggested but not mandatory, and may be chosen according to application needs.

Gaussian Frequency Shift Keying (GFSK) modulation is used to minimise transceiver complexity. The maximum bit rate is 1 Mbit/s. Maximum effective payload is lower because the different protocol layers require data payload for signalling to their corresponding layers in the unit with which the device is communicating. Actual data speed is 721 Kbit/s per piconet. Bluetooth is specified to operate with a maximum Bit Error Rate (BER) of 0.1%. This gives a figure for receiver sensitivity of −70 dBm as described in the Bluetooth specification.

1.4 Baseband Specifications

Baseband defines the physical RF link between the Bluetooth devices forming a piconet. The Bluetooth protocol uses a combination of circuit and packet switching. Slots can be reserved for Synchronous Connection Oriented (SCO) and Asynchronous Connectionless (ACL) packets. SCO link is mainly used for voice and ACL link is used for data and signally purposes. Each voice channels supports a 64 kb/s synchronous (voice) channel in each direction. Continuously Variable Slope Delta (CVSD) modulation is used for the speech coding. The asynchronous channel can support maximal 723.2 kb/s asymmetric (and still up to 57.6 kb/s in the return direction), or 433.9 kb/s symmetric. Each voice channel uses 64kbit/s synchronous link.

The available channels in the full 2.4 GHz ISM band is 79 RF channels spaced at 1 MHz. However, Japan, Spain and France have a smaller available bandwidth that has only 23 RF channels spaced at 1 MHz. The channel is represented by a pseudo-random sequence hopping through the 79 or 23 RF channels. The channel is divided into time slots, each 625 us in length. Each time slot represents a RF hop frequency. On the channel, information is exchanged through packets. Each packet is transmitted on a different hop frequency. The nominal hop rate is 1600 hops/s. All Bluetooth units participating in the piconet are time- and hop-synchronised to the channel. A Time-Division Duplex scheme is used for full-duplex transmission. A packet nominally covers a single slot but can be extended to cover up to five slots.

1.5 Network Topology

Bluetooth supports both point-to-point and point-to-multipoint connections. In point-to-multipoint connections, the channel is shared among several Bluetooth units. Two or more units sharing the same channels form a piconet. One Bluetooth unit acts as the master of the piconet, whereas the other units act as slaves. Up to seven slaves can be active in the piconet. In addition, many more slaves can remain locked to the master in a so-called parked state. These parked slaves cannot be active on the channel, but remain synchronised to the master. The channel access is controlled by the master for both active and parked slaves.

Multiple piconets with overlapping coverage areas form a scatternet. Each piconet can only have a single master. However, slaves can participate in different piconets on a time-division multiplex basis. In addition, a master in one piconet can be a slave in another piconet. The piconets shall not be time or frequency synchronised. Each piconet has its own hopping channel. *Figure 1.4* shows piconet topology for a single slave operation (a), a multi-slave operation (b) and a scatternet operation (c).

Figure 1.4: Network Topology (Specification of the Bluetooth System-Core v1.0B, 1999)

2 INDOOR RADIO CHANNEL

2.1 Introduction

Before we can investigate the Bluetooth wireless connectivity performance and test out the required link budget, we have to understand in particularly the radio wave propagation characteristics for indoor environment. Followed by modelling the indoor channel based on theories and/or statistical measurements.

Channel is defined as a link connecting a transmitter and a receiver, thus we can also treat all media as channels. By defining the indoor channel, we can answer and predict the expected radio wave outcomes and characteristics when propagated through a medium.

There are two main aspects in modelling an indoor channel and these are attributed to reflection, diffraction and scattering of the electromagnetic wave propagation. Firstly, we want to know how to determine the path loss by determining the indoor propagation model. Next we are interested to find out the phenomenon of the varying received signal strength (i.e. small-scale fading) that impairs the radio performance of the system.

The principles of the indoor radio wave propagation are described. The description focuses only on Bluetooth indoor radio channel that is necessary in carrying out the simulations and field experiments.

2.2 Indoor Environment

Bluetooth initial operating place is assumed mainly to be at home and/or at office. It is logical to say that office will have higher occupants, larger floor area and more findings of man-made object. With these challenging characteristics, office environment was selected to model the indoor channel in the simulation and experiment. Bluetooth radio is found to be non dispersive but flat fading in the indoor channel.

In an office, the movement of people and objects are likely to be slow and less often. Hence, this indicates a minimum or zero Doppler spread. In Singapore, the average floor area of an office is 900m^2, therefore, the distance of the transmission link is likely to be 30m. Consequently, the path loss analysis on the operating distance of Bluetooth device was based on minimum of 1m to maximum of 30m. (Please note that Bluetooth specifies that the transmission link should be at maximum range of 10m at 0dBm.) Owing to the radio wave's reflection, scattering and diffraction on the large numbers of man-made objects (e.g. gypsum board partition, metal locker, computers, concrete wall...etc.) in a confined and relatively small area; rapid fluctuation of the receiving signal strength over a short period of time or travel distance is normally observed. This phenomenon is known as multipath fading or "small-scale fading"(. Rappaport T. S, 1996, pp139). The received signal level can be constructive or destructive due to the characteristic of multipath fading signals arriving at the receiver's antenna.

2.3 Basic Propagation Mechanisms

All propagation models are subjected to the radio wave propagation. The diversity behaviours are generally credited by the optical theory on reflection, diffraction and scattering.

2.3.1 Reflection

Reflection occurs when an incidental radio wave hits upon an object that has very large dimensions when compared to the wavelength of the propagating wave. For example, reflections occur from the surface of the walls and ceilings. The angle, θ, is equal for the incidental wave and reflected wave.

Figure 2.1: Reflection Wave Characteristic

When a radio wave travels from one medium to another medium having different electrical properties, the wave is partially reflected and partially transmitted. However, if a radio wave hits on a perfect dielectric, part of the energy is transmitted into the second medium and part of the energy is reflected back into the first medium, and there is no loss of energy in absorption. And if the second medium is a perfect conductor, then all incident

energy is reflected back into the first medium without loss of energy. Thus, a perfect conductor such as metal will have higher signal losses when radio wave hit on it.

2.3.2 Diffraction

Diffraction occurs when the radio waves in the transmission path are obstructed by a surface that has sharp edges. The resultant waves from these surfaces are of two different characteristics. One is the reflected wave and the other appears behind the obstacle, giving rise to a bending of wave around the obstacle, even when a line-of-sight path does not exist between transmitter and receiver (diffracted wave). At high frequencies, diffraction, like reflection, depends on the shape and dimension of the object, as well as the amplitude, phase, and polarization of the incident wave at the point of diffraction.

Figure 2.2: Diffracted Wave Characteristic

Diffraction is used to explain the phenomenon of radio signals being propagated around the curved surface of the earth and propagated behind obstructions. The received signal strength measured at the obstructed (shadowed) region is usually weak but useful.

Freznel zone method is used to predict the shadowed received signal level. Freznel zones are defined by the diffraction loss as a function of the path difference around an obstruction. Freznel zones represent successive regions where secondary waves have a path length from the transmitter to receiver which are $n\lambda/2$ greater than the total path length of a line-of-sight path. The successive n^{th} Fresnel zones have the effect of alternately providing constructive and destructive interference to the total received signal.

2.3.3 Scattering

Scattering is seemed when the medium through which the radio wave travels consists of objects with sizes that are small compared to the wavelength and where the number of obstacles per unit volume is large. Scattered waves are created by rough surfaces, small objects or by other irregularities in the channel. For example trees, traffic lights and lamp posts create scattering of radio waves.

Figure 2.3: Scattered Wave Characteristic

The received signal is often stronger than what is produced by the reflection and diffraction models alone. This is because when a radio radio wave hits on a rough surface,

the reflected energy is spread out (diffused) in all directions due to scattering. The scatter waves provide additional radio energy at a receiver.

2.4 Path Loss Model

In the office environment, the radio wave propagation is strongly influenced by the interior layout (e.g. cubicle arrangement, rooms, machines...etc.), number of occupants and construction materials of the building (e.g. gypsum board partition, wood partition, concrete partition...etc.). "In general, indoor channels may be classified either as line-of-sight (LOS) or obstructed (OBS) with varying degrees of clutter. (Rappaport T. S., Aug 1998)

There are two different propagation models in predicting the path loss. They are either theoretical models or empirical models. Propagation models that predict the mean received signal strength from a distant transmitter are used to analyse the coverage area. These models are only valid for analysing path loss prediction and not for multipath fading. I had presented here the famous theoretical model i.e. Free Space Propagation Model and one empirical model i.e. Attenuation Factor Model created by Seidel.

Figure 2.4: Multipath Fading and Path Loss

By using path loss models to estimate the received signal level as function of distance, it becomes possible to predict not only the path loss but also the signal-to-noise for a mobile communication system. Signal-to-noise is used to measure the carrier frequency radio performance and is translated to Bit Error Rate (BER) to measure the baseband performance. Bluetooth specifies BER of 0.1%.

2.4.1 Free Space Propagation Model

The free space propagation model is most often used for the link budget analysis of the satellite communication and microwave system. It is used to calculate the receiver's received signal level when the transmission path is unobstructed and is line-of-sight from the transmitter. It is the most basic and useful model that predicts the free space loss over the transmitter-receiver separation distance. The free space power received by a receiver

antenna that is separated from a radiating transmitter antenna by a distance d is given by the Friis free space equation:

$$P_r(d) = \frac{P_t G_t G_r \lambda^2}{(4\pi)^2 d^2 L} \qquad \textit{Equation 2.1}$$

Where P_r is the received power that is a function of the transmitter-receiver separation. d. P_t is the transmitting power, G_t is the transmitter antenna gain, G_r is the receiver antenna gain, λ is the wavelength of the carrier frequency and L is the system loss such as cable loss, splitter loss...etc. A value of $L = 1$ indicates no loss in the system hardware.

The gain of an antenna, G, is related to its effective aperture, A_e, by:

$$G = \frac{4\pi A_e}{\lambda^2} \qquad \textit{Equation 2.2}$$

The effective aperture A_e is related to the physical size of the antenna and λ is related to the carrier frequency by:

$$\lambda = \frac{c}{f} \qquad \textit{Equation 2.3}$$

Where f is the carrier frequency in Hertz and c is the speed of light in meters/s.

The Friis free space equation shows that the received power decays with distance at a rate of 20 dB/decade.

An isotropic radiator is an ideal antenna that radiates power with units gain uniformly in all directions and is often used to reference antenna gains in wireless systems. The effective isotropic radiated power (EIRP) is defined as:

$$EIRP = P_t G_t \qquad\qquad \textit{Equation 2.4}$$

It represents the maximum radiated power available from a transmitter in the direction of maximum antenna gain.

The path loss (PL), which represents signal attenuation as a positive quantity measured in decibel (dB), is defined as the difference (in dB) between the effective transmitted power and the received power, and may or may not include the effect of the antenna gains. The path loss for the free space model when antenna gains are included is given by:

$$PL\,(dB) = 10\log\frac{P_t}{P_r} = -10\log\left|\frac{G_t G_r \lambda^2}{(4\pi)^2 d^2}\right| \qquad \textit{Equation 2.5}$$

When antenna has no gains, the antennas are assumed to have unity gain, and path loss is given by:

$$PL\,(dB) = 10\log\frac{P_t}{P_r} = -10\log\left|\frac{\lambda^2}{(4\pi)^2 d^2}\right| \qquad \textit{Equation 2.6}$$

The Friis free space model is only valid predictor for P_r for values of d that are in the far-field of the transmitting antenna. Also, it is clear that the equation does not hold for $d = 0$. Hence, a close-in distance, d_0, is used as a known received power reference point. The received power, $P_r(d)$, at any distance $d > d_0$, may be related to P_r at d_0. "The reference distance d_0 for practical systems using low-gain antennas in the 1-2 GHz region is typically chosen to be 1m in indoor environment." (Rappaport T.S., 1996, pp. 73) Thus, the received power in free space at a distance greater than d_0 is given by:

$$P_r(d) = P_r(d_0)\left|\frac{d_0}{d}\right|^2 \qquad d >= d_0 \qquad \textit{Equation 2.7}$$

The above equation is normally expressed in logarithm for mathematical calculation simplicity and the power, P_r, is in units of dBm. It is given by:

$$P_r(d)\,dBm = 10\log\left|\frac{P_r(d_0)}{0.001\ W}\right| + 20\log\left|\frac{d_0}{d}\right| \qquad d >= d_0 \qquad \textit{Equation 2.8}$$

Where $P_r(d_0)$ is in units of watts.

2.4.2 Attenuation Factor Model

The attenuation factor model created by Seidel is a better prediction of the path loss that includes the effect of building type as well as the variations caused by obstacles in an indoor environment. The attenuation factor model is given by:

$$PL(d)\,dB = PL(d_0)\,dB + 10n_{SF}\log(d/d_0) + FAF \qquad \textit{Equation 2.9}$$

Where n_{SF} represents the exponent value for the "same floor" measurement. Appropriate n value can be selected from *table 2.1* created by Seidel in his research work.

	n	σ (dB)	Number of locations
All Buildings:			
All locations	3.14	16.3	634
Same Floor	2.76	12.9	501
Through One Floor	4.19	5.1	73
Through Two Floors	5.04	6.5	30
Through Three Floors	5.22	6.7	30
Grocery Store	1.81	5.2	89
Retail store	2.18	8.7	137
Office Building 1:			
Entire Building	3.54	12.8	320
Same Floor	3.27	11.2	238
West Wing 5th Floor	2.68	8.1	104
Central Wing 5th Floor	4.01	4.3	118
West Wing 4th Floor	3.18	4.4	120
Office Building 2:			
Entire Building	4.33	13.3	100
Same Floor	3.25	5.2	37

Table 2.1: Path Loss Exponent and Standard Deviation for Various Types of Buildings (S. Y. Seidel and T. S. Rappaport, February 1992)

Then the path loss on a different floor can be predicted by adding an appropriate value of Floor Attenuation Factor (*FAF*) that can be selected from *table 2.2* (another hard work from Seidel). *FAF* may be replaced by an exponent that already considers the effects of multiple floor separation.

$$PL(d) \text{ dB} = PL(d_0) \text{ dB} + 10 n_{MF} \log(d/d_0) \qquad \text{Equation 2.10}$$

Where n_{MF} denotes a path loss exponent based on measurements through multiple floors.

Table 2.1 illustrates typical values of *n* for a wide range of locations in many buildings. It also illustrates how the standard deviation decreases as the average region becomes smaller and more site specific.

Building	FAF (dB)	σ (dB)	Number of locations
Office Building 1:			
Through One Floor	12.9	7.0	52
Through Two Floors	18.7	2.8	9
Through Three Floors	24.4	1.7	9
Through Four Floors	27.0	1.5	9
Office Building 2:			
Through One Floor	16.2	2.9	21
Through Two Floors	27.5	5.4	21
Through three Floors	31.6	7.2	21

Table 2.2: Average Floor Attenuation Factor in dB for One, Two, Three and Four Floors in Two Office Buildings (S. Y. Seidel and T. S. Rappaport, February 1992).

2.5 Link Budget Calculation

To determine the coverage and quality of a wireless communications system, it is important to calculate the receiver noise and Signal-to-Noise Ratio (SNR) at a receiver. SNR determines the link quality and probability of error (i.e. Bit Error Rate, BER) in the digital system. As a result, the ability to estimate SNR is significant for determining suitable transmitter powers or received signal level in various propagation conditions.

The signal level at a receiver antenna may be computed based on path loss equations. However, to compute the noise floor at the input of a receiver, it is necessary to know the gains (or losses) of each receiver stage, as well as the ambient noise temperature at the receiver antenna.

All electronic components inherently produce thermal noise that is observed at the detector output of a receiver. In order to refer the noise at the output of a receiver to an equivalent level at the receiver input terminals, the concept of Noise Figure (NF) is used and is defined as:

$$NF = \frac{\text{Measured noise power out of device at room temperature}}{\text{Power out of device if device were noiseless}}$$

NF is always greater than 1 and assumes that a matched load operating at room temperature is connected to the input terminals of the device.

Noise figure may be related to the effective noise temperature, T_e, of a device by:

$$T_e = (NF - 1)T_o \qquad\qquad Equation\ 2.11$$

Where To is ambient room temperature (typically taken as 300K, which corresponds to 27°C). Noise temperatures are measured in Kelvin, where 0K is absolute zero, or –273°C. Note that Te does not necessarily correspond to the physical temperature of a device.

A simple passive load (such as resistor) at room temperature transfers a noise power of:

$$P_n = kT_oB \qquad\qquad Equation\ 2.12$$

into a matched load, where k is Boltzmann's constant given by 1.38×10^{-23} Joules/Kelvin and B is the equivalent bandwidth of the measuring device. For passive devices such as transmission lines or attenuators operating at room temperature, the device loss (L in dB) is equal to the noise figure of the device that is,

$$NF = L \qquad\qquad \textit{Equation 2.13}$$

The concepts of noise figure and noise temperature are useful in communications analysis, since the gains of the receiver stages are not needed in order to quantify the overall noise amplification of the receiver. If a resistive load operating at room temperature is connected to the input terminals of a receiver having noise figure, NF, then the noise power at the output of the receiver, referred to the input, is

$$P_{out/Ref.in} = NFkT_oB \qquad\qquad \textit{Equation 2.14}$$

And the actual noise power out of the receiver is

$$P_{out} = GsysNFkT_oB \qquad\qquad \textit{Equation 2.15}$$

where G_{sys} is the overall receiver gain due to cascaded stages.

2.6 Small-Scale Multipath Propagation

Multipath in the radio channel creates small-scale fading effects. Small-scale fading or simply fading describes the rapid fluctuating of the received signal strength phenomenon over a short period of time of travel distance. Fading is the resulting effects at the receiver's antenna that had combined all the arriving signals. The combined signal can vary widely in amplitude and phase, depending on the distribution of the intensity and relative propagation time of the waves and the bandwidth of the transmitted signal.

Figure 2.5: Small-Scale Propagation Effect at Receiver's Antenna

The three important effects of fading are:

- Fast changes in signal strength over a small travel distance or time interval

- Random frequency modulation due to varying Doppler shifts on different multipath signals.

- Time dispersion (echoes) caused by multipath propagation delays.

Even when a line-of-sight exists, multipath still occurs due to reflections from the ground and surrounding structures. The incoming radio waves arrive from different directions

with different propagation delays. The signal received by the mobile at any point in space may consist of a large number of plane waves having randomly distributed amplitudes, phases and angles of arrival. These multipath components combine vectorially at the receiver antenna and can cause the signal received by the mobile to distort of fade. Even when a mobile receiver is stationary, the received signal may fade due to movement of surrounding objects in the radio channel.

2.6.1 Factors Influencing Small-Scale Fading

Many physical factors in the radio propagation channel influence small-scale fading. These include the following:

- Mulitpath propagation – The presence of reflecting objects and scatterers in the channel create a constantly changing environment that dissipates the signal energy in amplitude, phase, and time. These effects result in multiple versions of the transmitted signal that arrive at the receiving antenna, displaced with respect to one another in time and spatial orientation. The random phase and amplitudes of the different multipath components cause fluctuations in signal strength, thereby inducing small-scale fading, signal distortion, or both. Mulitpath propagation often lengthens the time required for the baseband portion of the signal to reach the receiver which can cause signal smearing due to intersymbol interference.

- Speed of the mobile – The relative motion between the transmitter and receiver results in random frequency modulation due to different Doppler shifts on each of the multipath components. Doppler shifts will be positive or negative depending on whether the mobile receiver is moving toward or away from the transmitter.

- Speed of the surrounding – If objects in the radio channels are in motion, they induce a time varying Doppler shift on multipath components. If the surround objects move at a greater rate than the mobile, then this effect dominates the small-scale fading. Otherwise, motion of surrounding objects may be ignored, and only the speed of the mobile need be considered.

- The transmission bandwidth of the signal – If the transmitted radio signal bandwidth is greater than the "bandwidth" of the multipath channel, the received signal will be distorted, but the received signal strength will not fade much over a local area (i.e., the small-scale signal fading will not be significant). The coherence bandwidth is a measure of the maximum frequency difference for which signals are still strongly correlated in amplitude. If the transmitted signal has a narrow bandwidth as compared to the channel, the amplitude of the signal will change rapidly, but the signal will not be distorted in time. Thus the statistics of small-scale signal strength and the likelihood of signal smearing appearing over small-scale distances are very much related to the specific amplitudes and delays of the multipath channel, as well as the bandwidth of the transmitted signal.

2.6.1.1 Doppler Shift

Due to the relative motion between the receiver and the transmitter, each multipath wave experiences an apparent shift in frequency. The shift in received signal frequency due to the motion is called Doppler shift, and is directly proportional to the velocity and direction of motion of the mobile with respect to the direction of arrival of the received multipath wave.

Consider a mobile moving at a constant velocity v, along a path segment having length d

between points X and Y, while it receives signals from a remote source S, as illustrated in

figure 2.6.

Figure 2.6: Doppler Effect

The difference in path lengths travelled by the wave form source S to the mobile at points

X and Y is $\Delta l = d\cos\theta = v\Delta t\cos\theta$, where Δt is the time required for the mobile to travel

from X to Y and θ is assumed to be the same at points X and Y since the source is

assumed to be very far away. The phase change in the received signal due to the difference

in path lengths is therefore

$$\Delta\phi = \frac{2\pi\Delta l}{\lambda} = \frac{2\pi v\Delta t}{\lambda}\cos\theta \qquad\qquad Equation\ 2.16$$

and hence the apparent change in frequency, or Doppler shift, is given by f_d, where

$$f_d = \frac{1}{2\pi} \frac{\Delta\phi}{\Delta t} = \frac{v}{\lambda} \cos\theta \qquad \textit{Equation 2.17}$$

Equation 2.17 relates the Doppler shift to the mobile velocity and the spatial angle between the direction of motion the mobile and the direction of arrival of the wave. It can be seen from *equation 2.16* that if the mobile is moving toward the direction of arrival of the wave, the Doppler shift is positive (i.e., the apparent received frequency is increased), and if the mobile is moving away form the direction of arrival of the wave, the Doppler shift is negative (i.e. the apparent received frequency is decreased). The maximum Doppler shift, f_m occurs for a wave coming from the opposite direction as the direction of the antenna is moving to. It has a frequency shift of $f_m = v / \lambda$.

The time varying phase shifts of individual reflected waves affect the received signal level at the antenna. Hence, Doppler effects determine the rate at which the received signal fluctuates.

2.6.1.2 Delay Spread

The time-dispersive indoor channel can be perceived to be time invariant linear response. Hence, the channel impulse response caused by mulitpath reflections looks like a series of pulses.

Figure 2.7: Impulse Response and Frequency Function of a Multipath Channel.

Due to the time-dispersive medium, the typical delay envelope e(t) of an impulse response at the reception occurs as shown in *figure 2.8*.

Figure 2.8: Delay Spread

The mean delay time T_d and the delay spread Δ can be calculated as

$$T_d = \int_0^\infty t \cdot e(t) \, dt \qquad\qquad Equation \; 2.18$$

and

$$\delta^2 = \int_0^\infty t^2 \cdot e(t) \, dt - T^2_d \qquad\qquad Equation \; 2.19$$

respectively, where e(t) is the resultant impulse signal received from an impulse signal $S_0(t) = a_0.\delta(t)$.

$$e(t) = a_0 \sum_{i=1}^{N} a_i . \delta(t - T_i) e^{-j\omega t} = E(t)e^{j\omega T} \qquad \qquad Equation\ 2.20$$

where T is the time delay, a_i is the reflection coefficient of the ith paths, and $\delta(t)$ is the impulse function, as shown in *figure 2.9*.

Figure 2.9: Delay Spread Profile

"The indoor delay spread is typically <0.1µs." (William C. Y. Lee, 1993). The previous values are unchanged for any operating frequency above 30MHz because above 30MHz the wavelengths are always much less than the sizes of human-made structures. A delay spread model can be expressed as

$$p(T_i) = \frac{1}{\Delta} \exp\left| -\frac{T_i}{\Delta} \right| \qquad \qquad Equation\ 2.21$$

where T_i is the time delay. This model is assumed by N equal amplitude reflected waves, most of which arrive closely earlier on. Very few arrive later, as shown in *figure 2.9A*. The distribution of delay spread $p(T_i)$ is shown in intervals. The two models are equivalent, but the model of *equation 2.21* is easier to use for mathematical manipulation.

Figure 2.9B shows also the delay profile that determines to what extent the channel fading at two different frequencies f_1 and f_2 are correlated. The maximum delay time spread is the total time interval during which reflection with significant energy arrive. The RMS (root-mean-square) delay spread is the standard deviation value of the delay of reflections, weighted proportional to the energy in the reflected waves.

By obtaining a large set of impulse responses in the indoor channel. The delay profile of the expected power per unit time received with a certain excess delay (typically $0.1\mu s$) is shown below

Figure 2.10: Typical Indoor Delay Profile

It can be seen that early reflections often arrive with almost identical power. This gives a fairly flat profile up to some time and a tail of weaker reflections with larger excess delay.

2.6.1.3 Coherent Bandwidth

In a time-dispersed medium the fades of two received envelopes will coincide in time if the frequency separation ΔF is small enough. This means that the ΔF is within the coherence bandwidth. If a coherence bandwidth can be found by choosing two frequencies that are far from the coherence bandwidth, we can cause the two received signals to fade independently. The coherence bandwidth is derived from a correlated function $R(\Delta f)$ of two fading signal envelopes at two frequencies f_1 and f_2 respectively,

$$R(\Delta f) = \langle s(f_1) \cdot s(f_2) \rangle \qquad \Delta f = |f_1 - f_2| \qquad \textit{Equation 2.22}$$

and $p(\Delta f)$ is a correlation coefficient after normalising $R(\Delta f)$, using the analog autocorrelation coefficient the coherence bandwidth (Bc) can be obtained as:

$$B_c = \Delta f_1 \qquad \textit{Equation 2.23}$$

We also can find a correlation coefficient form low random phases of two fading signals following the same steps as shown in *equation 2.22*. For two fading amplitudes to vary uncorrelately, the frequency separation should be greater than the coherence bandwidth B_c.

$$\Delta f > B_c = \frac{1}{2\pi\Delta} \qquad \textit{Equation 2.24}$$

The coherence bandwidth is different in situation in suburban and urban areas. Because their time delay spreads (Δ) are different due to different human-made structures in the mobile radio environment.

2.6.1.4 Intersymbol Interference

In a dispervsive medium the transmission rate R_b in a digital transmission is limited by the delay-spread phenomenon. Since Δ is the mean delay spread, the transmission rate should be based on the maximum delay spread, which can be about 2Δ. if low bit-error rate performance is required:

$$R_b < \frac{1}{2\Delta} \qquad Equation\ 2.26$$

In a real situation R_b would be determined from the required bit-error rate. which is based on the delay spread.

2.6.2 Types of Small-Scale Fading

In a dispersive medium, there are two kinds of spread: Doppler spread F and delay spread δ. Doppler spread F is spreading in frequency and delay spread δ is spreading in time. In strict sense all media are dispersive. However, we can classify a medium's characteristics based upon the signal duration T and the signal bandwidth W of a transmitted waveform in operation.

2.6.2.1 Non Dispersive Channels

A non dispersive but fading channel is created if these two kinds of spread F and δ meet the following conditions:

$$F \ll \frac{1}{T} \quad \text{and} \quad \delta \ll \frac{1}{W}$$

A non dispervise fading channel is also called a flat-flat fading channel. In many practical systems we choose the values of W and T so that the previous conditions are met and the system is in a non dispersive channel.

2.6.2.2 Time-Dispersive Channels

Some channels are dispersive in only in time, but not in frequency. For a time dispersive channel to exist, the following condition must hold:

$$\delta \gg \frac{1}{W} \quad \text{and} \quad \delta \gg T \quad \text{(dispersive in time)}$$

But

$$F \ll \frac{1}{T} \quad \text{(not dispersive in frequency)}$$

The illustrations of these time-dispersive channels are shown in *figure 2.11*. They are also called frequency-selective fading. This is because at the same time a signal could be faded

at one frequency but not necessarily at another. Sometimes they are called time-flat fading

channels.

Figure 2.11: Time Dispersive Channels, $\delta \gg 1/W$

2.6.2.3 Frequency-Dispersive Channels

Some channels are dispersive in frequency, but not in time. The following conditions are

expressed for frequency-dispersive channels:

$$F \gg \frac{1}{T} \quad \text{and} \quad F \gg W \qquad \text{(dispersive in frequency)}$$

But

$$\delta \ll \frac{1}{W} \qquad \text{(not dispersive in time)}$$

The frequency-dispersive channel is also called time-slective fading, since the channel

selectivity alters certain time segments of the transmitted wave-form. It is also called

frequency-flat fading, since all the constituent frequencies of the transmitted waveform are

modulated by the same functions. This frequency dispersive channel is illustrated in *figure 2.12.*

Figure 2.12: Frequency Dispersive Channel $F \gg 1/T$

2.6.2.4 Ricean Statistical Model

When there is a dominant stationary (non fading) signal component present, such as a line-of-sight propagation path, the small-scale fading envelope distribution is Ricean. In such situation, random multipath components arriving at different angles are superimposed on a stationary dominant signal. At the output of an envelope detector, this has the effect of adding a dc component to random multipath.

Just as for the case of detection of a sine wave in thermal noise, the effect of a dominant signal arriving with many weaker multipath signals gives rise to Ricean distribution. As the dominant signal becomes weaker, the composite signal resembles a noise signal which has an envelope that is Rayleigh. Thus the Ricean distribution degenerates to a Rayleigh

distribution when the dominant component fades away. The Ricean distribution is given by:

$$P(r) = \begin{cases} \dfrac{r.e^{-(r^2 + A^2)/2\sigma^2}}{\sigma^2} . I_0\left[\dfrac{Ar}{\sigma^2}\right] & \text{for } (A >= 0, r >= 0) \\[3ex] 0 & \text{for } (r < 0) \end{cases} \qquad \text{Equation 2.27}$$

The parameter A denotes the peak amplitude of the dominant signal and $I_0[.]$ is the modified Bessel function of the first kind and zero-order. The Ricean distribution is often described in terms of a parameter K which is defined as the ratio between the deterministic signal power and the variance of the multipath. It is given by $K = A^2/(2\sigma^2)$ or, in terms of dB

$$K(\text{dB}) = 10 \log \frac{A^2}{2\sigma^2} \text{ dB} \qquad \text{Equation 2.28}$$

The parameter K is known as the Ricean factor and completely specifies the Ricean distribution. As $A \rightarrow 0$, $K \rightarrow -\infty$ dB, and as the dominant path decreases in amplitude, the Ricean distribution degenerates to a Rayleigh distribution. *Figure 2.12* shows the Ricean pdf.

Figure 2.13: Probability Density Function of Ricean Distribution
K = -∞ dB (Rayleigh) and K = 6dB. For K >> 1, the pdf is Gaussian about the mean.

2.6.2.5 Rayleigh Statistical Model

The Rayleigh distribution is commonly used to describe the statistical time varying nature of the received envelop of a flat fading signal, or the envelop of an individual multipath component. It is well known that the envelop of the sum of two quadrature Gaussian noise signals obeys a Rayleigh distribution. The Rayliegh distribution has a probability density function given by:

$$P(r) = \begin{cases} \dfrac{r.e^{-r^2/2\sigma^2}}{\sigma^2} & \text{for } (0 <= r <= \infty) \\ 0 & \text{for } (r < 0) \end{cases}$$

Equation 2.29

Where σ is the rms value of the received voltage signal before envelope detection, and σ^2 is the time-average power of the received signal before envelope detection. The probability that the envelop of the received signal does not exceed a specified value R is given by the corresponding cumulative distribution function (CDF)

$$P(R) = Pr(r <= R) = \int_0^R p(r)\, dr = 1 - \exp\left[-\frac{R^2}{2\sigma^2}\right]$$

Equation 2.30

The mean value r_{mean} of the Rayleigh distribution is given by:

$$r_{mean} = E(r) = \int_0^\infty r p(r)\, dr = \sigma\left[\frac{\pi}{2}\right]^{1/2} = 1.2533\sigma$$

Equation 2.31

and the variance of the Rayleigh distribution is given by σ^2, which represents the ac power in the signal envelope.

$$\sigma^2_r = E(\,r^2) - E^2(\,r) = \int_0^\infty r^2 p(\,r)\,dr - \frac{\sigma^2 \pi}{2} \qquad\qquad Equation\ 2.32$$

$$= \sigma^2(\,2 - \pi/2\,) = 0.4292\sigma^2$$

The rms value of the envelope is the square root of the mean square of $\sqrt{2}\sigma$. The median

value of r is found by solving

$$\frac{1}{2} = \int_0^{r_{median}} p(\,r)\,dr \qquad\qquad Equation\ 2.33$$

and is

$$r_{median} = 1.177\sigma \qquad\qquad Equation\ 2.34$$

Thus the mean and the median differ by only 0.55 dB in a rayleigh fading signal. Note that

the median is often used in practise, since fading data are usually measured in the field and

a particular distribution cannot be assumed. By using median values instead of mean

values it is easy to compare different fading distributions which may have widely varying

means. *Figure 2.14* illustrates the Rayleigh pdf.

Figure 2.14: Probability Density Function of Rayleigh Distribution

2.7 Rayleigh Fading

Bluetooth is modelled for obstructed line-of-sight applications. Hence Rayleigh fading

channel gives the best description of the multipath fading phenomenon. The receiver's

antenna receives a large number, say N, reflected and scattered waves. As explained

before the resultant received signal level varies randomly and is caused by the constructive

or destructive of the signal combined at the antenna. This random variable can be

portrayed by Rayleigh probability distribution function.

Figure 2.15: Rayleigh Fading Resultant Signal Level

The phasor diagram in *figure 2.15* shows a set of scattered waves (in red), resulting a

Rayleigh fading signal level (in blue). If the phasor diagram is imagined to be rotating

with time and varying set of scattered waves, Rayleigh fading envelope signal level can be

plotted. Also the resulting vector may significantly change amplitude if individual

components undergo different phase shift caused by Doppler shift. The motion of the

antenna and the received signal level changes proportionally. Deep fade is usually

observed in the order of half a wavelength.

In case of an unmodulated carrier, the transmitted signal has the form

$$v(t) = \cos(\omega_c t + \psi)$$ *Equation 2.35*

The received unmodulated signal $r(t)$ can be expresses as

$$r(t) = \sum_{n=1}^{N} c_n \cos(2\pi f_c t + \psi + \phi_n + 2\pi \Delta f_n t)$$ *Equation 2.36*

An in-phase-quadrature representation of the form

$$r(t) = I(t) \cos\omega_c t - Q(t) \sin\omega_c t$$ *Equation 2.37*

can be found with in-phase component

$$I(t) = \sum_{n=1}^{N} c_n \cos(2\pi v f_c t / c \cos\alpha_n + \psi + \phi_n)$$ *Equation 2.38*

and quadrature phase component

$$Q(t) = \sum_{n=1}^{N} c_n \sin(2\pi v f_c t / c \cos\alpha_n + \psi + \phi_n)$$ *Equation 2.39*

When the antenna is stationary, $v = 0$. An in-phase-quadrature representation reduces to

$$I(t) = \sum_{n=1}^{N} c_n \cos(\psi + \phi_n)$$ *Equation 2.40*

and

$$Q(t) = \sum_{n=1}^{N} c_n \sin(\psi_l + \phi_n)$$ *Equation 2.41*

Thus, both the in-phase and quadrature component, $I(t)$ and $Q(t)$ can be interpreted as the sum of many (independent) small contributions. Each contribution is due to a particular reflection, with its own amplitude c_n and phase. For sufficiently many reflections (large N), the Central Limit Theorem now says that in-phase and quadrature components tend to a Gaussian distribution of their amplitude. $I(t)$ and $Q(t)$ appear to be independent and identically distributed (zero mean Gaussian distribution). When the antenna is set to zero, channel fluctuations no longer occur. Fading is due to motion of the antenna. An exception occurs if reflecting objects move.

2.7.1 Doppler Power Spectrum

The models behind Rayleigh of Rician fading assume that many waves arrive each with its own random angel of arrival (thus with its own Doppler shift), which is uniformly distributed within $[0, 2\pi]$, independently of other waves. Hence, Doppler power spectrum is used to compute the probability density function of the frequency of incoming waves signal strength. This leads to the U-shaped power spectrum for isotropic scattering

$$S(f) = \frac{1}{4\pi f_m} \frac{1}{\mathrm{sqrt}(1 - (f - f_c)2 / f_m 2)}$$ *Equation 2.42*

Where a unity local mean power is assumed.

Figure 2.16: Doppler Power Spectrum (U-shaped in Red, Flat in Blue)

The indoor channel is found to be slow fading (i.e. zero to minimum Doppler shift) and therefore observed a flat Doppler spectrum. Uniformity is observed across the frequencies rather than over angles of arrivals. "This type of spectrum is caused by random movements of scattering elements in the area of the communication path, from random movements of the transmitter or receiver causes." (W. R. Nichols II and M. G. Amin, August 2000)

3 Simulation and Field Experiment

3.1 Introduction

Before the simulation and experiment were carried out, the Bluetooth specifications were interpreted and translated into appropriate indoor channel. Simulation was done using Matlab to analyse the path loss and calculation done on fading phenomenon for Bluetooth indoor channel. The results were interpreted and investigated following the radio performance based on the parameters of:

- Link Budget Requirement

- Signal-to-Noise Ratio (SNR)

- Bit Error Rate (BER)

- Inter-Symbol-Interference (ISI)

Field experiments were then performed to verify the simulation results. The experiment's measurements collected were:

- Received signal level over the transmitter-to-receiver separation distance of 1m to 30m in obstructed line-of-sight situation.

- Received signal level over the transmitter-to-receiver separation distance of 1m to 10m in line-of-sight situation.

- Object attenuation factor.

3.2 *Simulation and Experiment Parameters*

Prior to the simulations and experiments, parameters were set up and required for the analysis and investigation works. The parameters are:

- Bluetooth radio specifications

- Bluetooth scene

- Indoor Channel Model

3.2.1 Bluetooth Radio Specifications

Summary of the Bluetooth radio specifications used in the parameters is:

- Carrier frequency – 2.4GHz

- Transmission power – 0 dBm (10 mW)

- No power control feature

- Receiver sensitivity - -70 dBm

- 1 Mbps (maximum transmission rate)

- Unity gain (omni-directional) antenna is used for all Bluetooth devices

- 6 dB noise figure at the Bluetooth device

3.2.2 Bluetooth Scene

It is very likely that Bluetooth will be used and become popular in the office. Businessman will use Bluetooth enabled device to exchange their electronic name card through wireless at the meeting. (This wireless connectivity is most probably at 1m to 10m line-of-sight situation.) This data will then be updated in their personal digital assistance's contact for

record and future reference. In another scenario, when an employee stepped into the office area, he is automatically logged into the company's intranet using the Bluetooth. (This wireless connectivity is most probably at 1m to 30m obstructed line-of-sight situation.) The applications are not limited to downloading of emails and synchronising his/her work schedule that may have been just updated and delegated by his/her superior the day after leaving the office.

Heavy home usage of Bluetooth is also very likely to happen but it is believe that the office applications mean more to the initial users. Thus, office environment was chosen as the indoor channel. When deciding on the technical issues, office environment provides more challenging factors than home environment that can influence the indoor channel propagation. This is due to the fact that there are more movement i.e. higher Doppler shift and objects i.e. more multipath fading that contributes to higher path loss and delay spread.

3.2.3 Indoor Channel Model

The indoor channel was modelled as non dispersive channel by the following prove:

For non dispersive channel is must satisfied the following criteria:

- $F \ll 1/T$ where F is Doppler spread and T is channel period.

- $\delta \ll 1/W$ where δ is the delay spread and W is bandwidth.

Given: Indoor delay spread, F, is typically $< 0.1 \times 10^{-6}$ sec

Channel duration, T, of Bluetooth is specified at 1×10^{-6} sec

"For Personal Communication Services (PCS) operating at 2GHz, it is recommended that most of the indoor pedestrian communicatiOn environments be modelled within the flat-spectrum model, with maximum Doppler frequency of 9.6Hz." (W. R. Nichols II and M. G. Amin, August 2000)

Now, we proved that the channel is non dispersive by

$$F(9.6\text{Hz}) \ll 1 / T(1 / 1 \times 10^{-6}) \ll 1\,\text{MHz}$$

$$\delta\,(0.1 \times 10^{-6}\,\text{sec}) \ll 1 / W\,(1 / 1 \times 10^{6}) \ll 1 \times 10^{-6}\,\text{sec}$$

The channel was also modelled as Rayleigh flat fading channel. (i.e. the amplitude fading varies in time is governed by the Rayleigh distribution.) For this, it need to be satisfying the conditions of

$B_s \ll B_c$ where B_s (Bluetooth specification is 1 MHz) is the signal bandwidth and B_c is the coherence bandwidth.

Assuming the frequency function correlation is above 0.5, then the coherence bandwidth is approximately

$$B_c \approx 1/5\sigma_\tau \approx 2\,\text{MHz}$$

Hence, it was proven that $B_s\,(1\,\text{MHz}) \ll B_c\,(2\,\text{MHz})$

The second condition was also proven by

$Ts \gg \sigma_\tau$ where Ts (Bluetooth specification is 1×10^{-6} sec) is the channel period and σ_τ (typically 0.1×10^{-6} sec) is the rms delay spread.

$1 \times 10^{-6} \gg 0.1 \times 10^{-6}$

Consequently, two particular models were exploited to study the Rayleigh flat fading indoor channel for Bluetooth office applications. The first model, attenuation factor model was used to predict the path loss. Next, the Rayleigh distribution was used to analyse the amplitude fading.

3.3 Analysis Works

We have defined previously the necessary parameters on the radio specifications, applications, office environment and indoor channel model. Now we proceed further to analyse the radio performance in the area of ISI and link budget that are inter-related to the BER, SNR, path loss model and receiving sensitivity.

3.3.1 Analysis of Inter-Symbol-Interference

Bluetooth bit rate is 1 Mbps, hence the bit duration is 1 μs. Given that speed of light is 3 x 10^8 m/s we obtained:

$$3 \times 10^8 / 1 \times 10^{-6} = 300m \quad \text{(one bit is 300 meters long)}$$

Thus, ISI occurs only if path difference between the transmitter and receiver were significant portions of 300 meters. This will not happen in our $900m^2$ office environment.

3.3.2 Analysis of Path Loss Model

The predictive models for fading and path loss used are:

- Path loss – Attenuation factor model (*equation 2.9*) with n = 3.3, this figure is reported for use in office environment with obstructed line-of-sight situation at 2.4GHz (H. Hashemi, pp.958, July 1993).

- Amplitude fading model, Rayleigh distribution, for obstructed line-of-sight situation.

3.3.3 Link Budget Analysis

The link budget analysis for meeting 0.1% BER (i.e. received sensitivity of –70dBm) is:

- Thermal Noise of Bluetooth

$$\text{Thermal Noise @ 1 MHz} \quad = kT_oB$$
$$= 1.38 \times 10^{-23} \times 300K \times 1 \times 10^6$$
$$= 4.14 \times 10^{-15}$$

$$\text{dBm} \quad = 10 \log (4.14 \times 10^{-15} \times 1000)$$
$$= -114 \text{ dBm}$$

where k is the Boltzmann's constant, B is the bandwidth and T_o is ambient room temperature in Kelvin (assumed to be 300K).

- Link Budget Margin (Maximum allowed path loss)

$$\text{Noise Floor @ Bluetooth device} \quad = -114 \text{ dBm} + 6 \text{ dB}$$
$$= -108 \text{ dBm}$$

For downlink:

$$\text{Link Budget Margin} \quad = \text{Noise Floor @ Bluetooth device - Transmitting power}$$
$$= -108 \text{ dBm} - 0 \text{ dBm}$$
$$= 108 \text{ dB}$$

The Bluetooth device is assumed to have 6 dB noise figure. This number is typical of a

GSM handphone.

For uplink:

        Receiver sensitivity = -70 dBm

        Link Budget Margin = Transmitting power – Receiver sensitivity
                              = 0 dBm – 70 dBm
                              = 70 dB

3.4 Simulation

The main objectives of the simulation were to use computer to calculate the receivable

signal strength at a given distance and to determine the fading effect.

From the free space loss model, Bluetooth device is able to operate up to 31 m. It is given

by:

        Since the receiver sensitivity is –70dBm, the maximum allowable path loss is
        therefore 70dB for transmitter power of 0dBm (see *Section 3.3*, link budget
        analysis, for detailed calculation).

        Free space loss   = 20 log $(4\pi d / \lambda)$

        Hence;   d ≈ 31 meters

This model is an ideal case (i.e. line-of-sight without fading effect). It is not sufficient to

predict the actual received signal strength that is influenced by multipath fading and the

signal loss caused by the obstructed objects and structures in the indoor channel. Thus,

attenuation factor model was used to predict the path loss. This model has considered the

factor of signal loss of objects at office floor. Fading model, Rayleigh distribution model was then graphed to get the probability of the predicted received signal due to fading effect.

3.4.1 Attenuation Factor Model Simulation

The following results were obtained by using Matlab. The appropriate Matlab script can be found in the appendix.
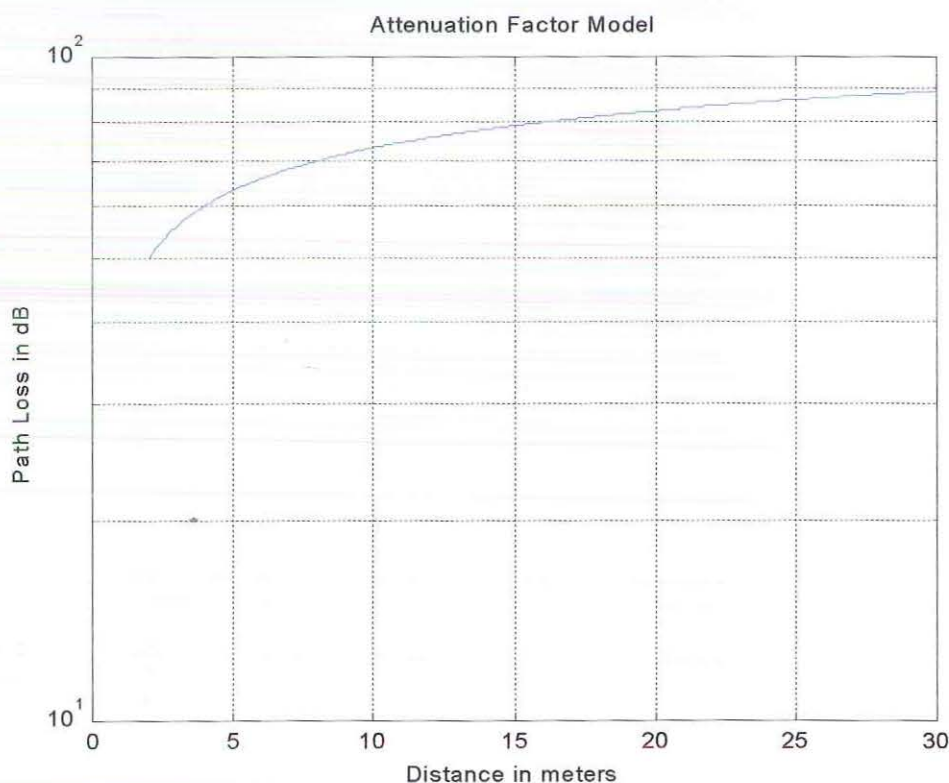

Figure 3.1: Attenuation Factor Model Plot

Since, I was interested only to calculate the path loss for the same floor, the exponent, FAF was ignored. The n_{SF} factor was taken as 3.3 (H. Hashemi, pp. 958, July 1993) for the same floor attenuation. The equation used was:

$$PL(d) \text{ dB} = PL(d_0) \text{ dB} + 10n_{SF}\log(d/d_0) + FAF$$

Where d was varying from 2m to 30m and d_0 was reference at 1m.

The tabulated path loss and received signal strength for 2m to 30m is shown in *table 3.1*.

The received signal strength was calculated by:

Received Signal Strength = Transmitting power with unity gain antenna – Path Loss
dBm   = 0 dBm – Path Loss

Nos.	Distance in Meters	Path Loss in dB	Received Level (dBm)
1	2	49.98	-49.98
2	4	59.91	-59.91
3	6	65.73	-65.73
4	8	69.85	-69.85
5	10	73.05	-73.05
6	12	75.66	-75.66
7	14	77.87	-77.87
8	16	79.78	-79.78
9	18	81.47	-81.47
10	20	82.98	-82.98
11	22	84.35	-84.35
12	24	85.59	-85.59
13	26	86.74	-86.74
14	28	87.80	-87.80
15	30	88.79	-88.79

Table 3.1: Predicted Path Losses and Received Signal Strength Over Designated Distance

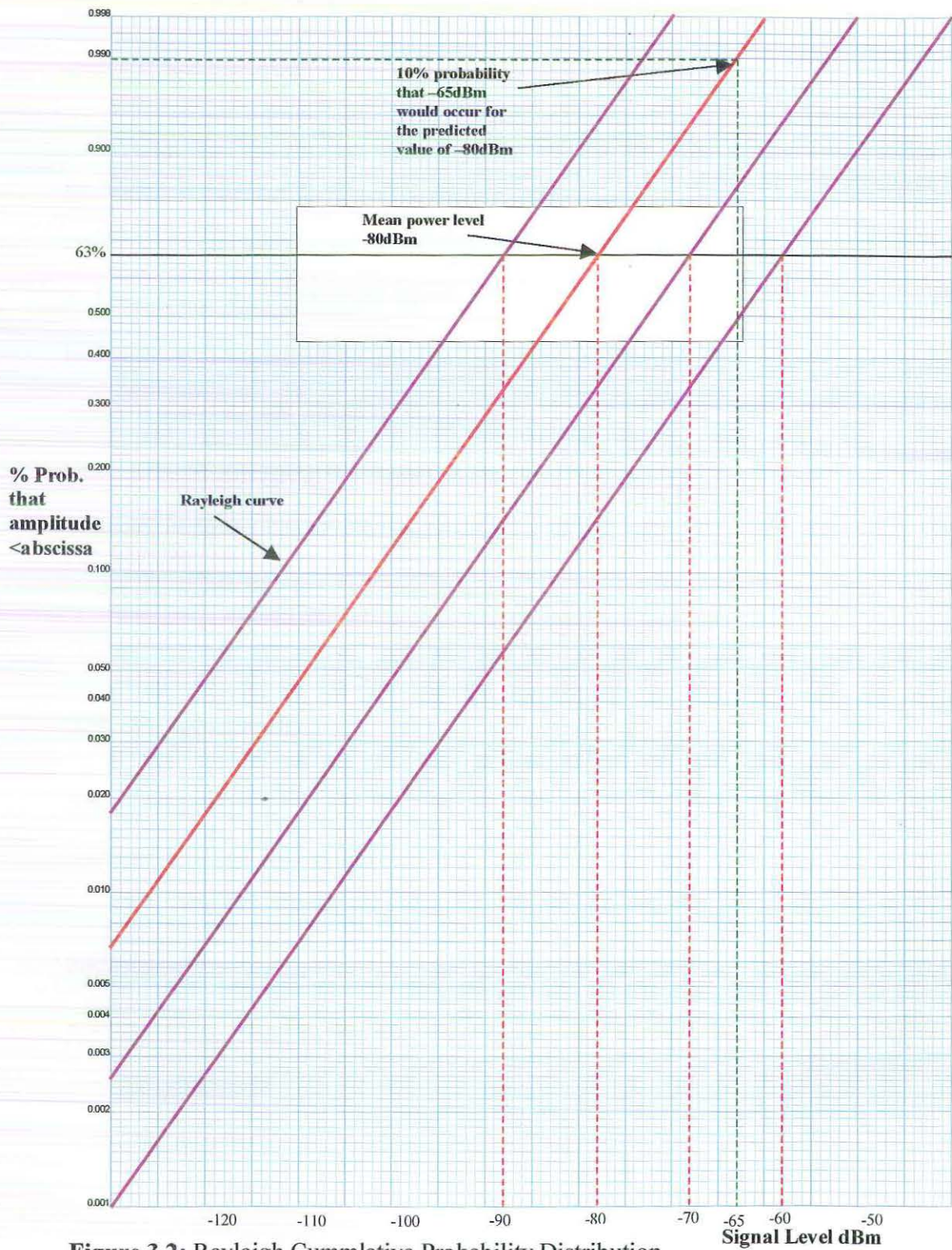## 3.4.2 Prediction of Amplitude Fading

Figure 3.2: Rayleigh Cummlative Probability Distribution

Rayleigh distribution was used to predict the behaviours of the rapid fluctuation of the received signal strength. It was reported by many researches that Rayleigh distribution gives the best prediction for flat fading, obstructed line-of-sight indoor channel fading.

As shown in *figure 3.2*, the Rayleigh graph paper could be easily used to interpret the probability of percentage on the arriving signal strength by fitting the Rayleigh curve on it. Since the predicted received signal strength shown in *table 3.1* only showed the path loss without fading consideration. With Rayleigh distribution, we could now say that 63% of the received signals would fall below the calculated received signals in *table 3.1*.

Only 37% of the received signals would exceed the predicted received signals. For example, in *figure 3.2*, at –80dBm predicted received signal level, 10% probability that it would be –65dBm.

3.5 Experiments

The main objectives of the experiments were to verify the simulation results and to measure the signal loss of objects found in the office.

Object signal loss experiment was conducted as it has significant influence on the link budget margin. Measurement of the office found objects were collected to give a guide of the type of signal loss due to blocked object. High signal losses will cause the Bluetooth not working probably even when the transmitter-receiver distance is short.

3.5.1 Object Signal Loss Experiment

This experiment is to measure the signal loss of objects when the 2.4 GHz Continuous Wave (CW) signal hit on it. The equipment needed for the experiment is:

- 01 x Marconi Instruments 9KHz to 2.4GHz signal generator 2024

- 01 x Advantest 9KHz to 3GHz spectrum analyser U3641

- Objects found in office

- 02 x Kathrien directional antenna 736 935

- 01 x Times Microwave systems RG 214 co-axial jumper cable (3.56dB loss)

- 01 x Huber Suhner RG214/U co-axial jumper cable (2.6dB loss)

3.5.2 Experiment Procedures

The experiment procedures were as follow:

1. First, the signal generator was calibrated.

2. Then directional antennas were fitted to the signal generator and spectrum analyser via the co-axial jumper.

3. The signal generator was set at 2.4GHz for transmission at 0dBm and the spectrum analyser was set to receive the signal at 2.4GHz.

4. Before measuring the intended object signal loss, the transmitting and receiving antennas were placed at 1m apart at line-of-sight in order to measure the reference received signal strength ($SS_{reference}$) in dBm.

5. Finally, the object signal loss was measured by placing the intended object in-between the transmitting and receiving antennas as mentioned in item 4.

6. Next, the measured signal strength ($SS_{measured}$) was recorded.

7. The Object Signal Loss (OSL) was then calculated by:

$$OSL = SS_{reference} - SS_{measured} \text{ (dB)}$$

8. Repeat the procedures from item 5 to 8 for different objects.

Figure 3.3: Set-up of the Object Signal Loss Experiment

Directional antennas were used so that the radiating wave fronts would concentrated at one direction, thus eliminating the possible effects of multipath fading. Omni-directional antenna can not be used as it has a 360 degree radiating pattern. The radio waves would travel at all directions from the transmitting antenna. Consequently, it may cause radio waves to be received at the antenna at unintended directions that were not the true wave that had passed through the testing object.

3.5.3 Receivable Signal Strength Experiment

This experiment was to verify the path loss model done in the simulation. Receivable signal strength was measured over the distance of 1m to 30m in the obstructed line-of-

sight situation and 1m to 10m line-of-sight. The measured points and office environment are shown in *figure 3.4*.
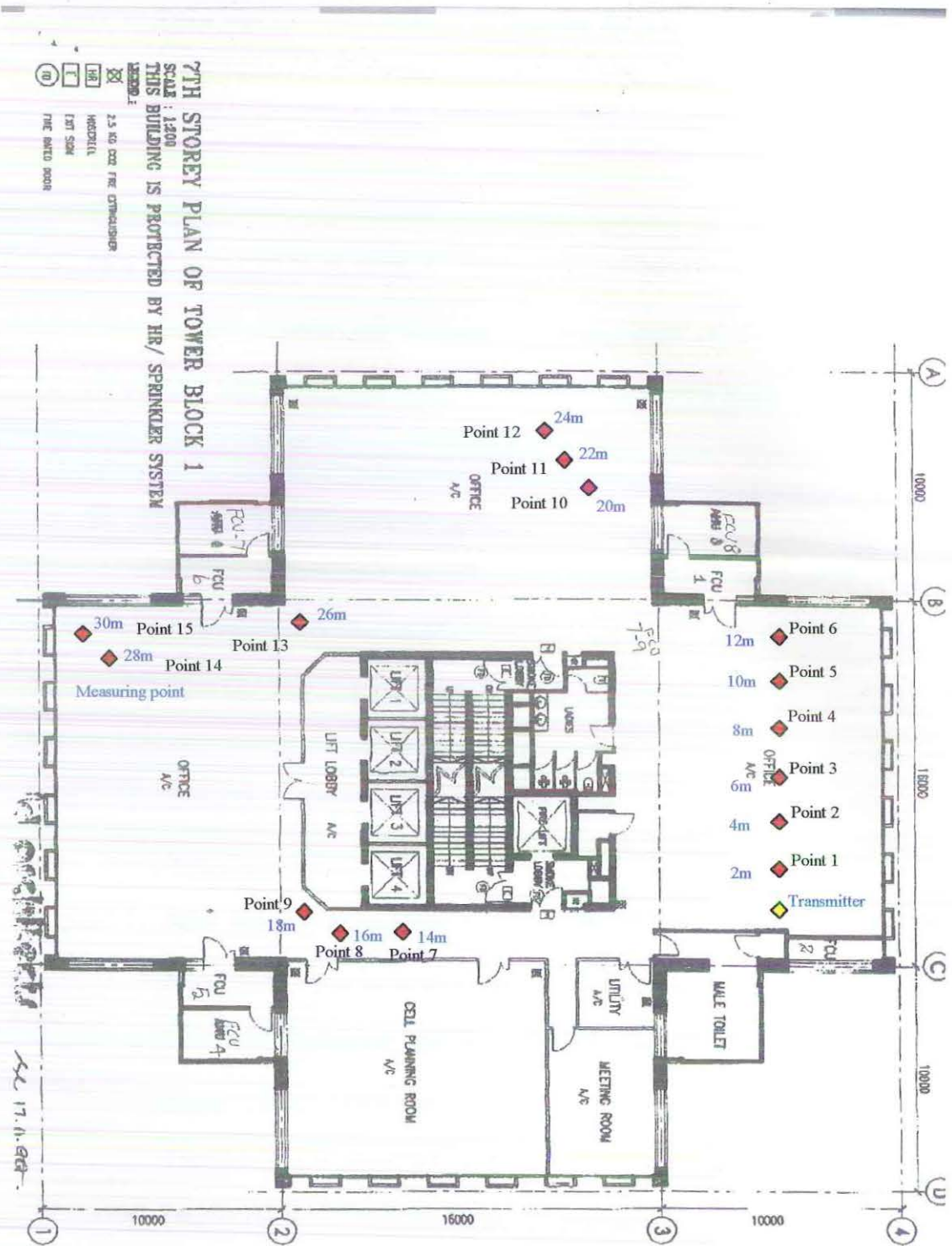
Figure 3.4: Office Floor Plan and Measuring Points

2.4GHz CW signal was generated in order to measure the predicted received signal. The equipments used for the experiment are:

- 01 x Marconi Instruments 9KHz to 2.4GHz signal generator 2024 (sensitivity level at −117dBm)

- 01 x Advantest 9KHz to 3GHz spectrum analyser U3641

- 01 x Times Microwave systems RG 214 co-axial jumper cable (3.56dB loss)

- 01 x Huber Suhner RG214/U co-axial jumper cable (2.6dB loss)

- 01 x Measuring tape

- 02 x Kathrein omni-directional antenna 736361

3.5.3.1 Experiment Procedures

The experiment procedures were as follow:

1. First, the spectrum analyser was calibrated.

2. Next, the co-axial jumper cables losses were measured at 2.4GHz.

3. After the above preparation works, the omni-directional antennas were fitted to the signal generator and spectrum analyser via the co-axial jumper.

4. The signal generator was set at 2.4GHz for transmission at appropriate power level of 0dBm and with offset of the cables loss measured in item 2. The spectrum analyser was set to receive the signal at 2.4GHz.

5. During the measurement, the signal generator and spectrum analyser were placed at 1m above from ground. This was because Bluetooth device would probably be placed on the table which had a height of 1m.

6. Received signal strength was measured and recorded accordingly to the measuring points in *figure 3.4*

.

3.6 Results, Comparison and Analysis

3.6.1 Object Signal Loss Experiment

Nos.	Office Objects	Signal Losses (dB)
1	Concrete wall 6 inches thick	8
2	Wooden door 3 inches thick	2
3	Metal cupboard filled with documents	35
4	Metal drawer cabinet	30
5	Cubicle partition 3 inches thick	1.3
6	Computer monitor with PVC chassis	16
7	Glass door	0.5
8	Gypsum ceiling board	1
9	Gypsum wall partition	2
10	Wooden table top	2
11	Computer metal chassis with motherboard	25
12	Printer	15
13	White board	15
14	Wooden Drawer Cabinet filled with documents	18

Table 3.2: Measurement of Office Objects Signal Loss @ 2.4 GHz

It can be seen from *table 3.2* that any objects consisted of metallic materials contribute to high signal loss. This was due to the fact that signal were mostly reflected by the conductive materials. Metal cupboard, computer monitor, computer chassis, printer and whiteboard showed the high signal loss from 15dB to 35dB. These losses could cause breakdown of the link budget i.e. the minimum receiver's sensitivity of the Bluetooth device could not be met and thus, device failed to work properly.

For non-metallic materials, the signal losses range from 0.5dB to 18dB. It was relatively smaller compared to the metallic materials. Radio waves were partly reflected and transmitted through the object. However, like the metallic materials, the signal loss increased when the object got thicker in depth.

3.6.2 Receivable Signal Strength Experiment

Points Nos.	Measuring Points in Distance (meters)	Measured Received Level dBm	Predicted Received Level dBm
1	2	-78.05	-49.98
2	4	-85.83	-59.91
3	6	-100.67	-65.73
4	8	-105.34	-69.85
5	10	-110.52	-73.05
6	12	-115.09	-75.66
7	14	-82.57	-77.87
8	16	-83.76	-79.78
9	18	-83.59	-81.47
10	20	-117	-82.98
11	22	-117	-84.35
12	24	-117	-85.59
13	26	-117	-86.74
14	28	-117	-87.80
15	30	-117	-88.79

Table 3.3: Measured and Predicted Received Signal Strength at Designated Locations

The measured and predicted received level were drastically different except for points 7, 8 and 9 which were in the line-of-sight situation. For points 10 to 15, we could only observed the constant level of −117dBm due to the limitation of the spectrum analyser.

The prime suspect of the extreme difference in the results was the high attenuation effect caused by the blocking objects in the obstructed line-of-sight. *Figure 3.5* showed the

experimental office environment. Although the picture showed only a portion of the office, the rest of the areas are also having similar set-up. It is mainly filled with low height cubicles in the center and occupied by metal cupboards at the walkways and high height cubicles at the window edge.

Figure 3.5: Office Environment

The transmitter was placed on top of the table at the extreme side of the office perimeter. Each receiving points at 1 to 6 were then placed at 1m high and 2m intervals away from the transmitter as shown in *figure 3.4*. As illustrated in *Figure 3.5*, the transmitter-receiver path was blocked by computers and printers. The placement of the transmitter and receiver were lower than the height of the obstructions. Hence, high attenuation was observed for these points. From the object signal loss experiment, the computer monitor had a signal loss of 16dB! Therefore for addictive signal losses through these equipments, the difference between the predicted received signal level and measured received signal level was from about 26dB to 34dB. It could not be contributed by multipath fading as through

inspection in *figure 3.2* the probability for the measured signal levels to happened were from 1.8% to 30%. It was a relatively small probability for it to be influential.

Points 7 to 9 measured results came very close to the predicted results. This could be due to that the transmitter-receiver path had a partially obstructed line-of-sight by a metal drawer cabinet only. The comparison of predicted and measured results for both path loss and fading were from 2dB to 5dB and from 50% to 60% respectively. The models proved to be accurate.

Measurements at points 10 to 15 went out of the range of the spectrum analyser receiver sensitivity. As seen in *figure 3.4*, these points were at another portion of the office layout. The line-of-sight paths from these points to the transmitter were severely attenuated by large and conductive objects such as the metal cupboards, concrete walls and lift cars. Again this showed that the path loss model was useless when there were high attenuation objects blocking in the obstructed line-of-sight situation.

4 CONCLUSION

4.1 Project Achievements and Contribution

The objectives were met accordingly to:

- An understanding of the indoor multipath propagation.

- An understanding of the Bluetooth specifications.

- Design, analysis and simulation of the small-scale fading and path loss model in Matlab and theory.

- An understanding and usage of the signal generator and spectrum analyser.

During the project, most of the time was spent on searching and reading about Bluetooth technology. The technology is although available in the late 1990's but not until December 2000 there are not more than four books available in the whole world. Shipment arrived in Singapore only on late January. Prior to acquiring the books, I depended a lot on surfing the Internet to learn about the technology.

There were limited resources (especially laboratory equipment) available to me. I had to spend quite considerable time to search and get temporary loan of any available equipments. Although there were many favours offered from my colleagues, I could only managed to get limited equipment. Consequently, the project objectives were shaped by these factors.

It can be concluded from the simulation results that at 0dBm, Bluetooth operates up to 8m. However the experiment results showed that Bluetooth failed to operate at all the measuring points. This was mainly due to that the antennas were placed very low and blocked by high attenuation objects in the obstructed line-of-sight. Hence, *Table 3.1* serves as a guide for Bluetooth users to avoid high attenuation objects. And Bluetooth user is advise to use the device at a higher height.

In the office, the obstructed line-of-sight can be easily overcome if the Bluetooth devices are operating at a height of 1.5m. This height is observed to have less influencing obstructed line-of-sight. This will improved the received signal level since high losses are found for common desktop objects such as computer's chassis and monitor. If not, do not place active Bluetooth device directly towards metallic objects.

4.2 Comments and Recommendations for Future Research

Although the experiment was done on the unmodulated continuous wave and not the FH-CDMA modulated carrier, it had proven accurate results for the predictive path loss model. My findings here focused more on the link budget analysis, as this is the basic and most important factor to consider when designing a wireless communication link.
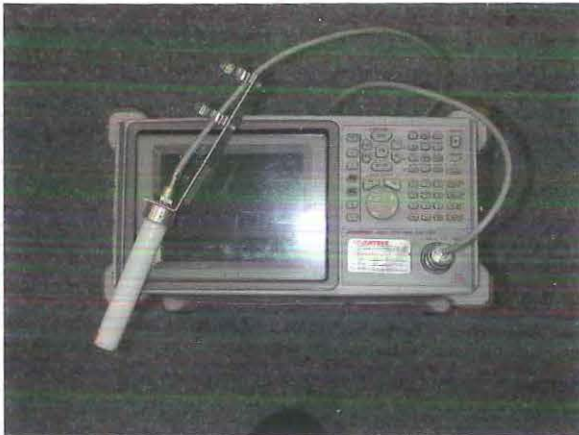
In actual fact, Bluetooth specifications on the radio and baseband provided the necessary techniques to combat the multipath fading effect. For example, error detection, frequency hopping, short data transmission, speech coding, retransmission protocol and power

control. Hence the mean received signal strength will be higher than what can be measured by this experiment.
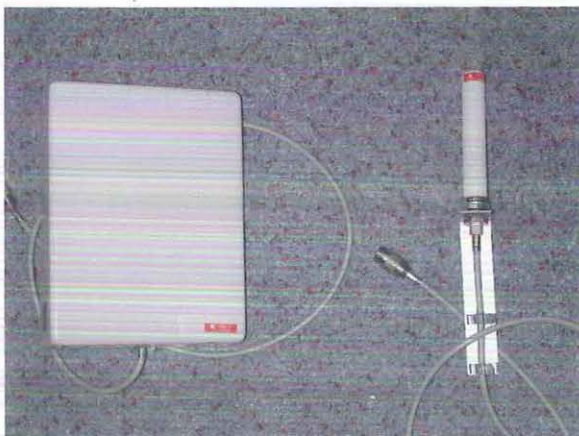
It is noted that every indoor environment has its own unique layouts and objects. Hence, there cannot be a 100% accurate model available for describing the indoor channels. However, we can follow up with channel impulse response experiment at site to ascertain the accuracy of the model for that channel.

For that reason, it is highly recommended that a channel impulse response experiment to be set up in order to best describe the indoor channel with measurements. It will also be interesting to study the interference between the same 2.4GHz ISM devices such as the wireless LAN (IEEE802.11b).

APPENDIX

Advantest 9KHz to 3GHz
spectrum analyser U3641

Kathrein omni-directional antenna
736361

Kathrien directional antenna 736
935

Marconi Instruments 9KHz to
2.4GHz signal generator 2024

Matlab code for Attenuation Factor Model

```
%Attenuation Factor Model

d0 = 1; %1 meter is used for close reference distance

d = 2:0.05:30; % d is the varying distance from 2m to 30m

freq = 2.4*10^9; % carrier frequency at 2.4GHz

lamda = 3*10^8/freq; % wavelength of the carrier frequency

PL0 = 20*log10(4*pi*d0 / lamda); % path loss at d0 distance

n = 3.3; % same office floor attenuation factor

PL = PL0 + 10*n*log10(d/d0); % attenuation factor path loss prediction

semilogy(d, PL); % plot semi log graph

xlabel('Distance in meters');
ylabel('Path Loss in dB');
title('Attenuation Factor Model');
grid on
```

BIBLIOGRAPHY

Bluetooth Overview [WWW document]. URL http://www.digianswer.com

Bluetooth Technology: The Convergence of Computing and Communications [WWW document]. URL http://www.gsmdata.com/cannes99/cannespaper.htm

Bluetooth Tutorial [WWW document]. URI. http://www.infotooth.com/tutorial.htm

Mettala, R (Aug 1999).Bluetooth Protocol Architecture version 1 [WWW document]. URL http://www.bluetooth.com/developer/whitepaper/whitepaper.asp

Specification of the Bluetooth System-Core v1.0B (1999) [WWW document]. URL http://www.bluetooth.com/developer/specification/specification.asp

Specification of the Bluetooth System-Profiles v1.0B (1999) [WWW document]. URL http://www.bluetooth.com/developer/specification/specification.asp

Technology: Bluetooth, [WWW document]. URL http://www.option.com/techno/bluetooth01.htm

Bray and Sturman (2001). Bluetooth: Connect Without Cables.
Prentice Hall PTR.

Nathan J. Muller (2000). Bluetooth Demystified.
McGraw-Hill Telecom.

William C. Y. Lee (1993). Mobile Communications Design Fundamentals (2nd Edition).
Wiley-Interscience.

Rappaport T. S. (1996). Wireless Communications: Principles and Practice.
. Prentice Hall PTR.

Rappaport T. S. (August 1989). Characterisation of UHF Mulitpath Radio Channels in Factory Buildings. IEEE Transactions on Antennas and Propagation, Vol. 37, No. 8, pp. 1058 – 1069, August 1989.

H. Hashemi (July 1993). The Indoor Radio Propagation Channel. Proceedings of The IEEE, Vol. 81, No. 7, pp. 943 – 968, July 1993.

W. R. Nichols II and M. G. Amin (August 2000). Modeling Systems Based on Bluetooth Wireless Connectivity. Microwaves & RF Magazine, pp. 121 – 134, August 2000.

Saleh and R. Valenzula (February 1987). A Statistical Modeling For Indoor Mulitpath Propagation. IEEE Journal On Selected Areas In Communications, Vol. 5, pp. 128 – 137, February 1987.

R. Ganesh and K. Pahlavan (June 1991). Statistical Modeling And Computer Simulation Of Indoor Radio Channel. IEEE Proceedings, Vol. 138, pp. 153 – 161, June 1991.

David K. Cheng (1989). Field and Wave Electromagnetics (2nd Edition). Addison Wesley.

T. Zwick, C. Fischer, D. Didascalou and W. Wiesbeck (January 2000). A Stochastic Spatial Channel Model Based on Wave-Propagation Modeling. IEEE Journal On Selected Areas In Communications, Vol. 18, No. 1, pp. 6 – 14, January 2000.

S. Y. Seidel and T. S. Rappaport (November 1994). Site-specific Propagation Prediction for Wireless In-Building Personal Communication System Design. IEEE Transaction on Vehicular Technology, Vol. 43, pp. 879 – 891, November 1994.

H. Hashemi (September 1993). Impulse Response Modeling of Indoor Radio Propagation Channels. IEEE Journal On Selected Areas In Communications, Vol. 11, pp. 967 – 978, September 1993.

J-F. Frigon, B. Daneshrad, J. Putnam, E. Berg, R. Kim, T. Sun and H. Samueli (March 2000). Field Trial Results for High-Speed Wireless Indoor Data Communications. IEEE Journal On Selected Areas In Communications, Vol. 18, pp. 297 – 308, March 2000.

T. S. Rappaport, S. Y. Seidel and K. Takamizawa (May 1991). Statistical Channel Impulse Response Models for Factory and Open Plan Building Radio Communication System Design. IEEE Transaction on Communications, Vol. 39, pp. 794 – 807, May 1991.

S. Y. Seidel and T. S. Rappaport (February 1992). 914 MHz Path Loss Prediction Models for Indoor Wireless Communications in Mulitfloored Buildings. IEEE Transactions on Antennas and Propagation, Vol. 40, pp. 207 – 217, February 1992.